

P. HANDZLIK\*, K. FITZNER\*

## ELECTRONIC PROPERTIES OF ANODIC OXIDE FILMS ON TITANIUM IN PHOSPHATE BUFFERED SALINE SOLUTION AND ARTIFICIAL SALIVA DETERMINED BY EIS METHOD

### ZASTOSOWANIE ELEKTROCHEMICZNEJ SPEKTROSKOPII IMPEDANCYJNEJ DO OKREŚLENIA WŁAŚCIWOŚCI ELEKTRONICZNYCH ANODOWYCH WARSTW TLENKOWYCH NA TYTANIE W ROZTWORZE SOLI FIZJOLOGICZNEJ BUFOROWANEJ FOSFORANAMI I SZTUCZNEJ ŚLINY

In the present work investigations of electronic properties of anodic oxide films on titanium were carried out. Two different solutions, namely PBS with pH=2.9 and artificial saliva with pH=5 were used. Oxide films were produced by using potentiostatic anodization of the metal. To analyse the properties of the films, Electrochemical Impedance Spectroscopy (EIS) was applied. The principles of this method were given in the introduction of the present paper. Two properties of the oxide films were derived: a density of charge carriers and a flat band potential. To derive these parameters Mott-Schottky dependence was applied. Donor density was found to be similar independently on the solution used. In turn, flat band potentials were found to be  $-0.144$  V vs. SCE in PBS solution, and  $-0.285$  V vs. SCE in artificial saliva. The obtained values confirmed the dependence of the flat band potential on pH of the solution.

*Keywords:* titanium, anodic oxide films, EIS, Mott-Schottky plot, flat band potential, donor density

W pracy wykonano badania mające na celu określenie właściwości elektronicznych warstw tlenkowych wytworzonych na tytanie w roztworach fizjologicznych. Do badań użyto dwóch roztworów: roztworu soli fizjologicznej buforowanego fosforanami (PBS) o pH równym 2.9 i roztworu sztucznej śliny o pH 5. Warstewki zostały wytworzone poprzez potencjostatyczne anodowanie tytanu. Jako metodę badawczą użyto Elektrochemiczną Spektroskopię Impedancyjną, która została dokładnie opisana we wstępie pracy. Określono dwie właściwości charakteryzujące warstwy tlenkowe tzn. gęstość nośników ładunku i potencjał płaskiego pasma. Do wyznaczenia tych wielkości użyto zależności Mott-Schottky'ego. Z przeprowadzonych eksperymentów wyznaczono gęstości donorów, które były podobne w przypadku obu roztworów. Potencjały płaskiego pasma wyniosły odpowiednio dla warstw tlenkowych w roztworze PBS  $-0,144$  V vs. NEK oraz  $-0,285$  V vs. NEK w roztworze sztucznej śliny. Wartości tych potencjałów potwierdziły zależność potencjału płaskiego pasma od pH roztworu.

## 1. Introduction

Titanium dioxide in its various forms is extensively used in different fields of science and engineering due to its specific properties like low absorption coefficient, high refractive index and large dielectric constant.  $\text{TiO}_2$  films can be used as electrochromic materials [1], for optical coatings [2, 3], as dielectrics [4], in lithium-ion batteries [5], dye-sensitized solar cells [6, 7] as well as an insulator for applications to memory cell capacitors and thin gate insulators in VLSI [4]. The hydrophilic and photocatalytic behavior of  $\text{TiO}_2$  films with the anatase phase allows to create products like easy-to-clean surfaces, 'self-cleaning' windows, antifogging glass, self-sterilizing and antibacterial tiles, pho-

tocatalytic air and water purification devices [8].  $\text{TiO}_2$  films are also used as a protection of metallic biomaterials due to good biocompatibility with the human body [9, 10].

$\text{TiO}_2$  films can be directly synthesized by a variety of techniques such as aerosol pyrolysis [11], chemical vapor deposition [4, 12], electrodeposition [10, 13, 14], and sol-gel processing [7, 15]. Most of them result in the formation of amorphous or crystalline anatase.

In our work  $\text{TiO}_2$  films were investigated in the relationship to the application of titanium as a biomaterial because  $\text{TiO}_2$  provides excellent corrosion resistance of Ti. This property results from  $\text{TiO}_2$  structure and its transport properties connected with it. It is known that  $\text{TiO}_2$  behaves like n-type semiconductor [16]. It is a very

\* LABORATORY OF PHYSICAL CHEMISTRY AND ELECTROCHEMISTRY, FACULTY OF NON-FERROUS METALS, AGH UNIVERSITY OF SCIENCE AND TECHNOLOGY, 30 MICKIEWICZA AVE., 30-059 CRACOW

important factor in analyzing the passivity of titanium, since the conductivity of TiO<sub>2</sub> films decides about the exchange reaction with the environment. The parameters which usually describe semiconductors are charge carrier densities, dielectric constant, and flat band potential. Thus, to analyze the influence of different conditions on these parameters, a reliable experimental method must be available. Such a method, which allows to obtain these parameters, is called Electrochemical Impedance Spectroscopy (EIS). This method was used in this study to derive Mott-Schottky plots, from which the electronic properties of anodic oxide films formed on titanium can be obtained.

The main goal of this work is to present the EIS method as a versatile technique able to characterize transport properties of anodic oxide films.

## 2. Characterization of EIS method

Impedance spectroscopy used in electrochemistry is a very powerful tool to study not only the charge transfer kinetics, but also the structure and properties of the interface (also multi-layered). Thus, it seems to be reasonable to describe briefly the principles of this method.

When sinusoidally varying voltage with constant frequency is applied to the electric circuit, the way the resulting current varies with time depends on the circuit. To analyse this response it is useful to represent the waveform by vector – like quantity called “phasors”. The amplitude of the voltage  $\mathbf{V}$  can then be represented by the radius of the circle, and the sinewave can be generated by the projection of the point moving around the circumference onto y-axis. Then at a given time:

$$V = \mathbf{V} \cdot \sin\omega t. \quad (1)$$

It is now easy to add two different voltages by adding the amplitudes in the same way vectors are added. However, since the two sinewaves did not need to start at the same moment, there may be an angular difference  $\phi$  between them, which is added to all values of  $\omega t$ . One may say that two waveforms are out of phase by the angle  $\phi$ , called the phase angle. On the plane they can be depicted as two vectors, but without definite direction. In fact, one of them must serve as the reference from which the phase angle can be drawn to the other. That’s why in the electric circuit theory they got the name “phasors”.

The circuit to which the time – dependent voltage is applied can contain resistors (which dissipate energy and are known from d.c. circuit theory) and so-called reactive circuit elements: capacitors and inductors (which store energy). These new elements have no true resistance. Let’s take the capacitor as an example. Alternating

current flows through the capacitor though no electrons actually pass it. If charge  $Q$  is stored on the capacitor resulting in a voltage  $V$  across it, the relationship which connects these two quantities is:

$$\frac{Q}{V} = C \quad (2)$$

where constant  $C$  is called capacitance.

It is easy to show that sinusoidal variation in voltage results in a current which is equal to:

$$\frac{dQ}{dt} = i = C \cdot \frac{dV}{dt} = (\omega C \mathbf{V}) \cos \omega t = \mathbf{I} \cos \omega t. \quad (3)$$

According to eqs.(1) and (3) current and voltage have the same frequency, but their amplitudes are separated by the angle  $\pi/2$ . We say that current leads the voltage by  $\pi/2$ . If voltage amplitude is drawn along x-axis on the phasor diagram, then the current amplitude is perpendicular to it. The ratio of voltage amplitude to current amplitude is equal to:

$$\frac{\mathbf{V}}{\mathbf{I}} = \frac{1}{\omega \cdot C} = X_C \quad (4)$$

which is called reactance. This looks like Ohm’s Law but it is important to notice that, contrary to the resistance, reactance is frequency dependent. Also, it should be remembered that depending on circuit elements respective phasors will be at various angles to each other, which must be taken into account during phasor’s addition. If, for example, the circuit is composed of the resistor and capacitor in series, and voltage generator connected to the circuit is represented by eq. (1), then the current and voltage just in the resistor are in phase:

$$\mathbf{V}_R = \mathbf{I} \cdot R. \quad (5)$$

But the current in the circuit, being the mixture of resistive and reactive components, must be shifted relatively to the generator voltage by the unknown angle  $\phi$ , which is between  $\pi/2$  and zero. Consequently, voltage across the resistor is given by  $v = \mathbf{I} R \sin(\omega t + \phi) = \mathbf{V}_R \sin(\omega t + \phi)$ . This means that on the phasor diagram (Fig. 1) the current in the circuit leads the generator voltage by angle  $\phi$ . If the generator voltage is drawn along x-axis, then the relative position of two other phasors corresponds to the scheme shown in Fig. 1.

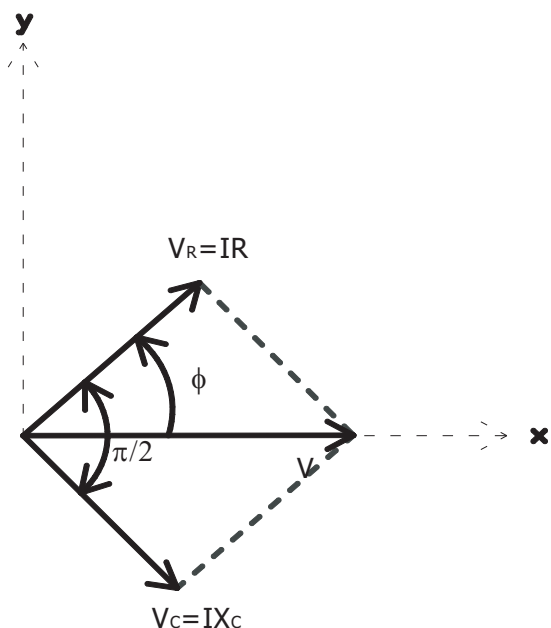


Fig. 1. Phasor diagram

This means that generator voltage is the sum of phasors:

$$\mathbf{V}^2 = \mathbf{V}_R^2 + \mathbf{V}_C^2 = (\mathbf{I}R)^2 + (\mathbf{I}X_C)^2 \quad (6)$$

from which the following relation can be obtained:

$$\mathbf{V} = \mathbf{I} \cdot \left( R^2 + \frac{1}{\omega^2 C^2} \right). \quad (7)$$

The ratio of the amplitudes of the voltage and current is called impedance  $Z$ :

$$\frac{\mathbf{V}}{\mathbf{I}} = Z = \left( R^2 + \frac{1}{\omega^2 C^2} \right). \quad (8)$$

Equation (8) relates the amplitudes of  $\mathbf{V}$  and  $\mathbf{I}$  but gives no information about relative phases of these two quantities. That's why phase angle of the impedance is needed. Unknown phase angle of the impedance can now be determined as  $\text{tg } \phi = X_C/R$ .

Summarizing, circuits having different components exhibit impedance  $Z$ , which must contain frequency dependent as well as frequency independent terms. However, phasor analysis of more complicated circuits can be very difficult since it is difficult to keep track of relative positions of all phasors. But, the fact that one needs two numbers to characterize the impedance (i.e. its modulus and the phase angle) allows us to express it as a complex number:

$$\mathbf{Z} = |\mathbf{Z}| e^{j\phi} = |\mathbf{Z}| \cos \phi - j |\mathbf{Z}| \sin \phi = Z_{\text{Re}} - j Z_{\text{Im}}. \quad (9)$$

In eq. 9,  $\mathbf{Z}$  is a complex impedance operator, which relates  $\mathbf{V}$  and  $\mathbf{I}$  phasors. When this operator of the circuit

is known one can deduce the impedance of the circuit which is simply the modulus of the complex impedance. Using this analytical tool, vector-like addition of phasors corresponds to the addition of complex numbers. However complicated the circuit, we can assign complex impedance to the reactive components:

- $j\omega L$  to inductors,
- $\frac{1}{j\omega C}$  to capacitors,

(where  $j = \sqrt{-1}$ ) while all resistors have real resistance  $R$ .

Next, one can apply all the usual rules of d.c. circuit theory to find complex impedance operator. It's about time to demonstrate this procedure in the case of simple electrochemical circuit. The general assumption is that the whole electrode system is electrically equivalent to the electric circuit and the analysis of the electrode phenomena is possible with the aid of this circuit. In Fig. 2a an interface between metallic electrode and the electrolyte is shown.

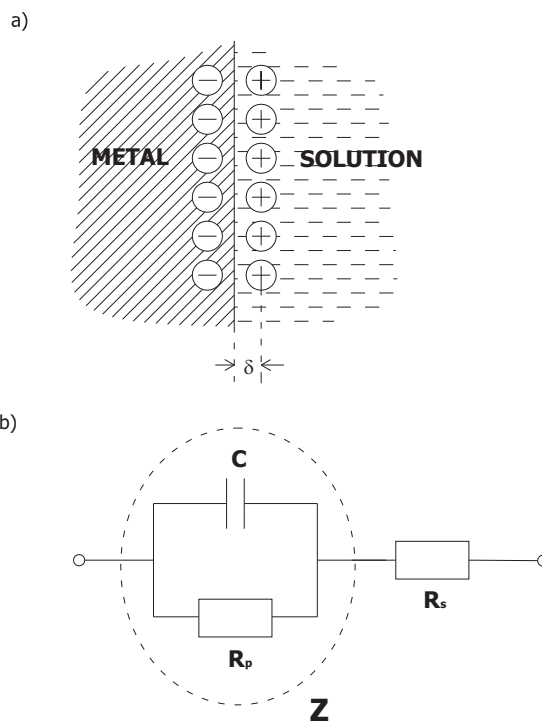


Fig. 2. a) metallic electrode immersed in a solution, b) equivalent electrical circuit

If the electron transfer reaction takes place, the interphase  $\delta$  is a region which can be envisaged as the leaking capacitor. In terms of the equivalent electrical circuit (Fig. 2b) the double layer is equivalent to electric capacitor and electrons going over double layer are equivalent to charge transfer resistance in parallel with the capacitor. Capacitor  $C$  and resistance  $R_t$  in parallel make reactive circuit characterized by the impedance  $Z$ . Far from the interface there is a resistance  $R_s$  of the

solution, which is in series with this reactive circuit For resistances in series we have:

$$Z_{total} = R_s + Z \quad (10)$$

where  $Z$  of the reactive elements in parallel is:

$$\frac{1}{Z} = \frac{1}{R_p} + \frac{1}{X_C} = \frac{1}{R_p} + j\omega C. \quad (11)$$

Consequently, the impedance for the whole circuit  $Z_{total}$  can be expressed as:

$$Z_{total} = R_s + \frac{R_p}{1 + j\omega CR_p}. \quad (12)$$

In order to obtain impedance magnitude it is necessary to multiply complex impedance by its complex conjugate  $Z^*$ . For complicated expression, complex conjugate can be obtained by simply changing  $j$  to  $-j$  everywhere in this expression. Then, impedance magnitude  $|Z|$  for a given frequency is equal to  $(ZZ^*)^{1/2}$  which is impedance vector length on the complex plane.

The usual procedure is to rearrange eq. 12 in order to obtain:

$$\begin{aligned} Z_{total} &= R_s + \frac{R_p}{1 + j\omega R_p C} \frac{(1 - j\omega R_p C)}{(1 - j\omega R_p C)} = \\ &\left[ R_s + \left( \frac{R_p}{1 + \omega^2 R_p^2 C^2} \right) \right] - j \left[ \frac{\omega R_p C}{1 + \omega^2 R_p^2 C^2} \right] = \\ Z_{Re} - jZ_{Im} &= a - jb. \end{aligned} \quad (13)$$

Plotting  $-Z_{Im}$  part against  $Z_{Re}$  part on the complex plane we mark coordinates of the vector, whose length for a fixed frequency is  $|Z|$  and the angle with the real axis  $\phi = \arctg(Z_{Im}/Z_{Re})$ . Changing the frequency gradually one may obtain the spectrum of points on this plane, which produce characteristic semicircle called Nyquist or Cole-Cole plot [17, 18]. Analyzing the behavior of eq.13 in the frequency limits one may find that for  $\omega \rightarrow 0$  impedance  $Z_{total} \rightarrow R_s + R_t$  while for  $\omega \rightarrow \infty$  impedance  $Z_{total} \rightarrow R_s$ . These two points mark the beginning and the end of the semicircle on the real axis in Fig. 3a, and indicate how charge transfer resistance and solution resistance can be derived. Also, for the frequency for which  $Z_{Re} = Z_{Im}$  (the radius of the semicircle is perpendicular to the real axis) one can obtain:

$$Z_{Im} = \frac{1}{\omega_{max} C} \quad (14)$$

and the system exhibits purely capacitive behavior from which the capacitance of the double layer can be obtained. In this way possible steps of the electrochemical reaction can be identified in terms of the experimentally

determined parameters of the equivalent circuit. It was probably Randles [19] who suggested for the first time that the performance of the electrochemical cell can be represented by an equivalent circuit of  $R$  and  $C$  elements. Pioneering works of Epelboin et al. [20, 21], Armstrong et al. [22, 23] and Sluyters et al. [24, 25] followed.

During the applications of EIS to electrochemical systems the impedance is obtained from experiments. Modern potentiostats possess a special module called Frequency Response Analyzer (FRA) which allows continuous measurements of impedance while varying frequency of the input signal. The results of measurements are displayed in the complex plane as  $Z_{Im}$  vs.  $Z_{Re}$ . Then, the main problem consists in finding the model circuit which is equivalent to the whole electrode system. Since the rate of electrochemical processes at the electrode/electrolyte interface may be influenced by the charge transfer, diffusion, resistance of the electrolyte as well as the structure of the interphase region the problem to be solved is the identification of these separate steps in terms of individual circuit elements.

Several different situations at the interface are shown in Fig. 3a-e as an example, together with equivalent circuits and corresponding complex plane plots. In real systems however the picture is rarely as ideal as that shown in Fig. 3 since the results usually show deviations from an ideal semicircle. The main problems which can be encountered are as follows:

- "arcs" can be rotated due to surface inhomogeneity, roughness, surface morphology, some physicochemical processes. The impedance of the system must be described by the empirical function called frequency dispersion function

$$Z = \frac{R_t}{1 + (\omega CR_t)^\alpha} \quad (15)$$

where  $\alpha$  ( $0 < \alpha < 1$ ) is connected to the angle of rotation by  $(1 - \alpha)\pi/2$  [26]. Another typical distributed circuit element is constant phase angle element (CPE) denoted by symbol  $Q$ . Its impedance is described by the formula

$$Z_Q = \frac{1}{Y_0(j\omega)^n} \quad (16)$$

where  $Y_0$  is a preexponential factor, which is a frequency-independent parameter;  $n$  is the exponent, which defines the character of the frequency dependence ( $-1 \leq n \leq 1$ ). With  $n$  equal to unity,  $Y_0$  is an ideal capacitance [27]. Impedance  $Z_Q$  is widely used in electrochemical simulation of assorted complicated objects also for the description of processes that occur at interfaces in anodic oxide layers.

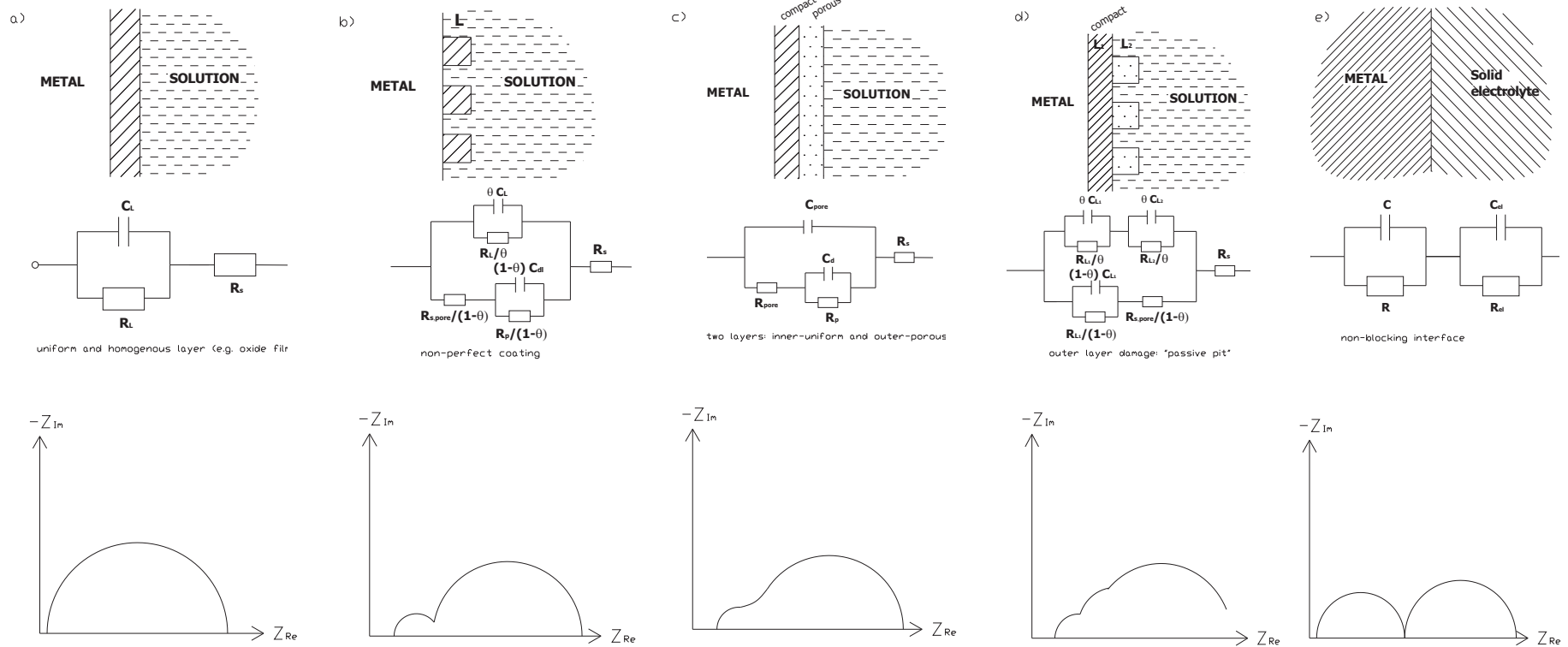


Fig. 3. Different situations at the interface, equivalent electrical circuits and corresponding complex plane plots

- “arcs” can overlap due to complicated interphase structure and there may be a problem how to split them into different parts connected to the circuit. Another attractive method used to interpret the results is that by means of Bode plots [31], in which impedance modulus and phase angle are shown as functions of  $\log(\text{frequency})$ . Sometimes this method provides more information about circuit elements.
- surface reactions may result in characteristic spiral-like shape of recorded impedance which corresponds to the appearance of the inductive element in the equivalent circuit [21].

Fortunately, advances in these two fields help to minimize the errors which can be made during interpretation of the obtained results:

1. unprecedented progress in structural analysis made in the field of material science allows literally “to see” what’s going on at the interface, and this information helps enormously to design proper equivalent circuit elements,
2. introduction of fast computers and availability of commercial software (e.g. EQIVCT [28], LEVM/LEVMW [29], Zview [30]) provides fast solution for the chosen equivalent circuit.

More detailed information about EIS technique can be found in comprehensive elaboration of Barsoukov and Macdonald [31]. In this paper we demonstrate how the determination of the capacitance can be used to derive electronic properties of the oxide film grown by anodization of the metal surface.

### 3. Experimental

#### 3.1. Samples

The specimens were made of titanium rod and sheet (Ti Grade 2 – impurity: O = 0.25% max, N = 0.03% max, C = 0.08% max, H = 0.015% max, Fe = 0.3% max). They were mechanically polished to a mirror-like surface by a 0.025  $\mu\text{m}$  alumina abrasive. After polishing, they were cleaned with soap and ethanol.

Before each experiment they were ultrasonically cleaned in acetone for 10 minutes and then in deionized purified water (Mili Q system, Milipore Corp.) also for 10 minutes. After cleaning the samples were mounted in a PVC holder. The exposed surface was a circle of 0.283  $\text{cm}^2$  geometrical area. The roughness factor  $\gamma$  determined from roughness measurements for these samples was circa 1.01.

#### 3.2. Cell and electrolytes

All experiments were performed in a three-electrode electrochemical cell containing about 45  $\text{cm}^3$  of elec-

trolyte. A platinum wire in the form of a spring was used as counter electrode. A saturated calomel electrode (SCE) Radiometer XR100 was the reference electrode and the working electrode was a titanium specimen. Additionally, in all EIS measurements a platinum wire was used immersed in the solution close to the SCE connected through a capacitor (0.1 – 1  $\mu\text{F}$ ) to the reference electrode connector of the potentiostat. This was done to reduce possible problems at high frequencies caused by the reference electrode. The experimental temperature was about  $21 \pm 1^\circ\text{C}$ .

All measurements were performed using the artificial saliva (Fusayama-Meyer solution) pH 5, and phosphate-buffered saline PBS pH 2.9. Solutions were prepared from pure analytical-grade compounds supplied by Sigma-Aldrich and deionized purified water (18  $\text{M}\Omega\cdot\text{cm}$ , MiliQ system, Milipore Corp.). The compositions of solutions are presented in Table 1. Electrolytes were not de-aerated to model the availability of oxygen in the physiological environment. The pH of each solution was measured before and after each experiment using Mettler DL 21 Titrator with the electrode Mettler Toledo DG-111-SC.

TABLE 1  
Composition of solutions used in experiments

Compound	Concentration in $\text{g}/\text{dm}^3 \pm 0.01 \text{ g}/\text{dm}^3$	
	Artificial saliva pH = $5 \pm 0.1$	PBS pH = $2.9 \pm 0.1$
NaCl	0.4	8
KCl	0.4	0.2
CaCl <sub>2</sub>	0.6	–
NaH <sub>2</sub> PO <sub>4</sub> ·H <sub>2</sub> O	0.69	–
Na <sub>2</sub> HPO <sub>4</sub>	–	3.6
KH <sub>2</sub> PO <sub>4</sub>	–	1.4
Urea	1	–
HCl*	–	to adjust pH

\* concentrated – 37%

#### 3.3. Experiments

To produce TiO<sub>2</sub> films titanium surface was anodized for 1h at the following potentials: 0.2V, 1.5V, 3V, 5V, 7V, 9V vs. SCE. After each anodization the impedance measurement was performed in order to obtain capacitance of the film. Also, the native oxide films formed after 1h immersion in solutions were investigated. The EIS measurements were performed on the titanium sample with produced TiO<sub>2</sub> at different potentials from –0.3 V to 1 V with the step 0.1 V. We obtained at each potential an impedance spectrum which was measured from 100 kHz to 5MHz in the potentiostatic mode using 10 mV voltage perturbation. To perform all these measurements Autolab PGSTAT12 was used. From the

obtained spectra the capacitance of the film was obtained and it was next used to construct Mott-Schottky plot, from which donor densities and flat band potential were calculated.

### 4. Results

In Fig. 4a an example of potentiodynamic curves is presented. They have been traced in the various solutions

mentioned earlier in the range of potentials from  $-2$  V to  $8$  V versus SCE with the scan speed  $-10$  mV/s. On this base we have chosen potentials to form oxides on the titanium surface. Also, we have obtained the stationary potentials, and these potentials are presented in Fig. 4b on the E-pH diagram for titanium based on [32]. As one can see they are in the passive range, which means that the surface of electrodes is covered with passive oxide film.

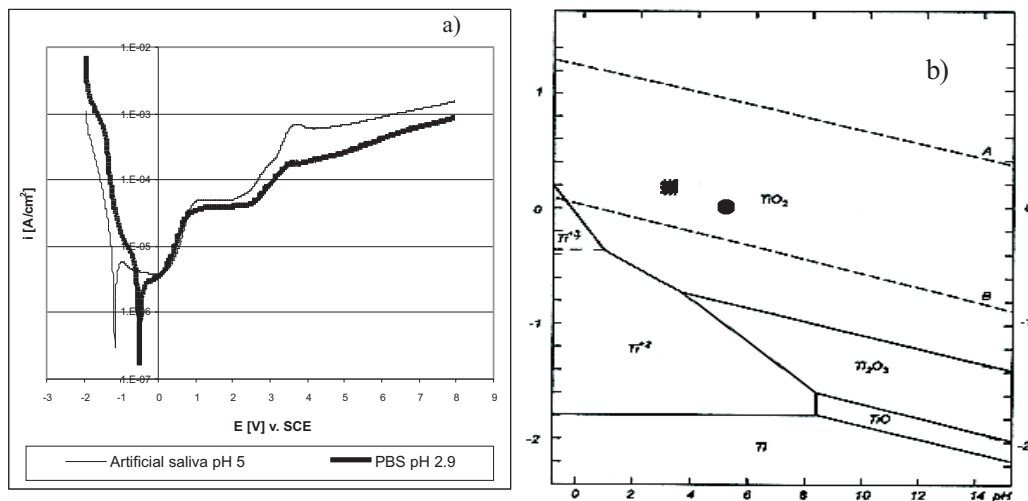


Fig. 4. a) Potentiodynamic curves for titanium in two different solutions b) E-pH diagram for titanium (based on [32]) with the stationary potentials (■ – PBS pH = 2.9 and ● – artificial saliva pH = 5)

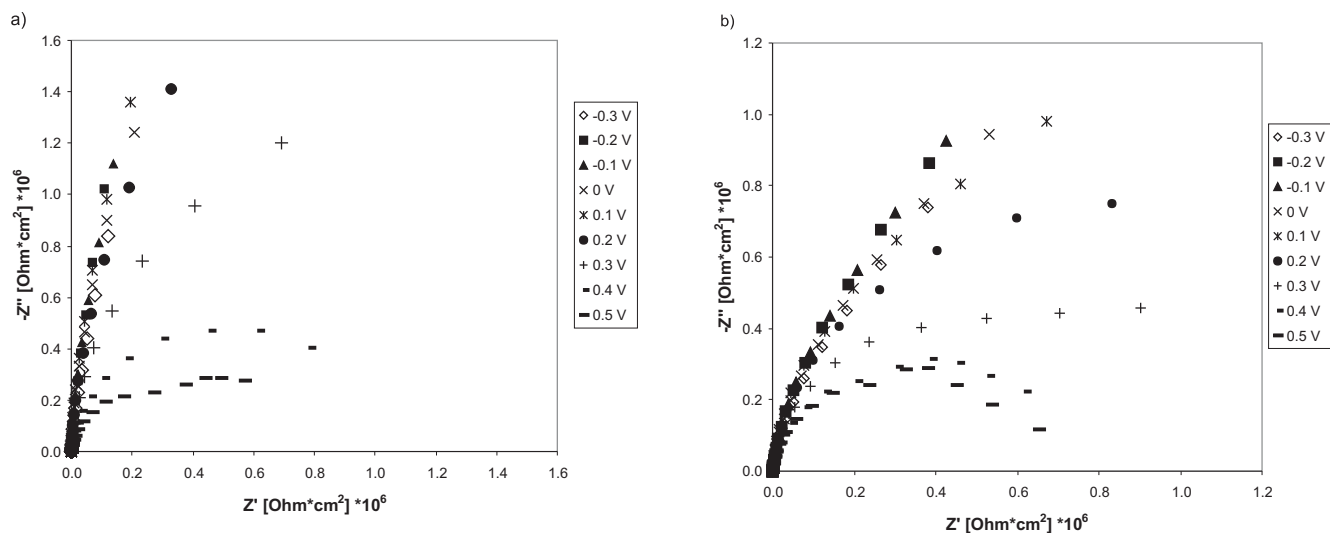


Fig. 5. Nyquist plots obtained for oxides formed at 0.2 V in a) PBS pH = 2.9 and b) artificial saliva pH = 5

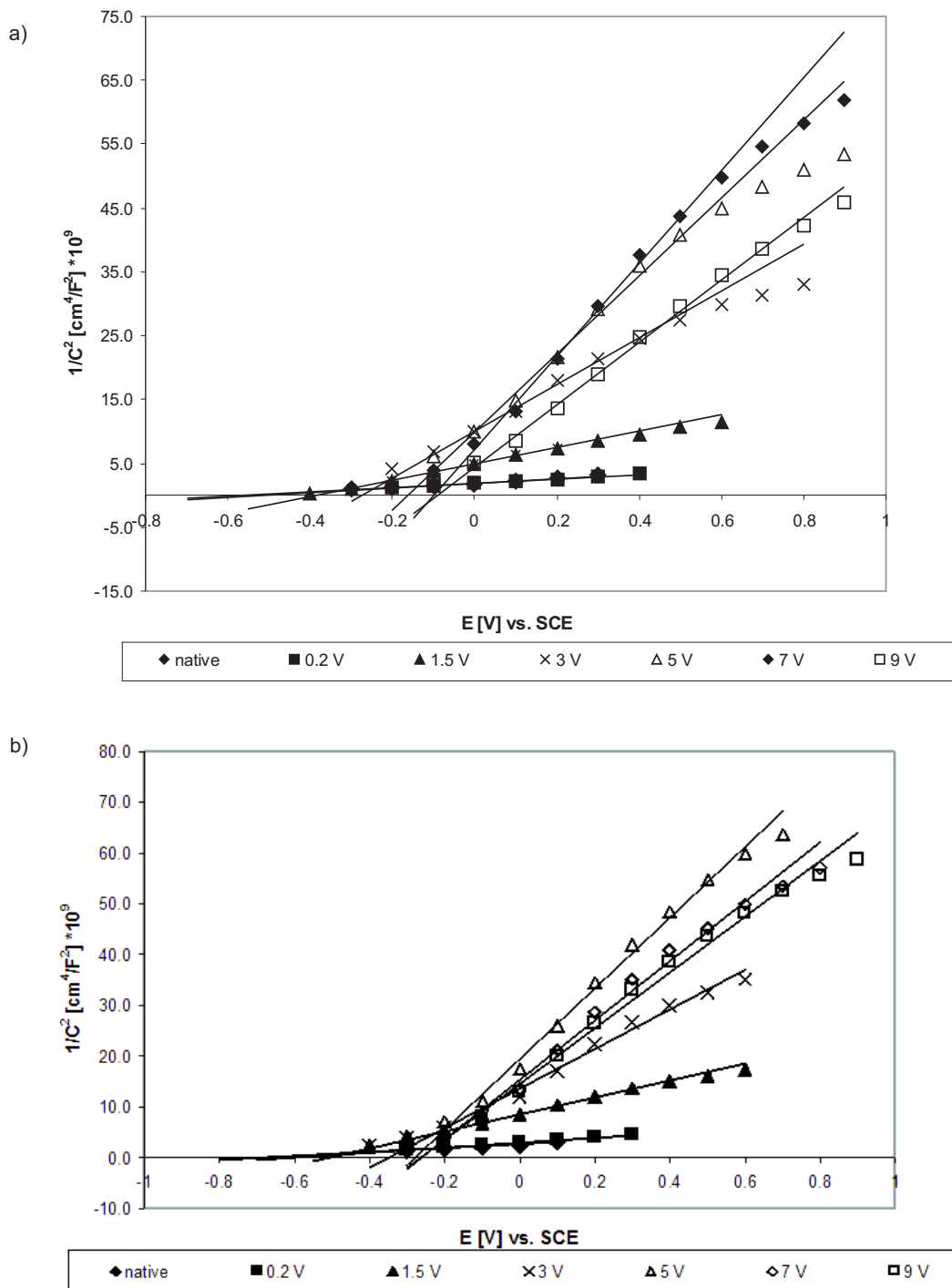


Fig. 6. Mott-Schottky plots for oxides formed at different potentials in a) PBS pH = 2.9 and b) artificial saliva pH = 5

Next, obtained films were investigated using EIS technique. Figures 5a and 5b show examples of Nyquist plots obtained under different potentials in two chosen solutions: PBS and artificial saliva. The Nyquist plots for films formed at other potentials were similar and have the same character. Using these plots and equivalent circuit

presented in Fig. 3a the capacitance  $C$  of oxide films was calculated and used to derive Mott-Schottky plots i.e.  $1/C^2$  vs.  $E$  dependences, which are presented in Fig. 6a and 6b.

The extended Mott-Schottky equation is presented below [33].

$$\frac{1}{C^2} = \frac{2}{e\epsilon\epsilon_0 N_d} \left( E - E'_{fb} - \Delta E - \frac{kT}{e} \right) \approx aE + b \quad (17)$$

$$E_{fb} = E'_{fb} + \Delta E \quad (18)$$

where:  $C$  – experimental capacity referred to the unit area,  $e$  – electron charge =  $1.602 \cdot 10^{-19}$  C,  $\epsilon$  – dielectric constant,  $\epsilon_0$  – electrical vacuum permittivity =  $8.85 \cdot 10^{-12}$  F/m,  $k$  – Boltzmann number =  $1.38 \cdot 10^{-23}$  J/K,  $T$  – temperature,  $E$  – experimental potential,  $E'_{fb}$  – experimental value of flat band potential,  $E_{fb}$  – true flat band potential obtained by correction of  $E'_{fb}$  by the potential drop  $\Delta E$  in the Helmholtz layer,  $N_d$  – donor density.

Using the Mott-Schottky equation (17) and the results shown in Fig. 6a and 6b parameters of linear equations were calculated and from the obtained values of the slope and intercept the donor densities and  $E'_{fb}$  values were derived.

We have used dielectric constant equal 50 as an average value for  $\text{TiO}_2$  taken from literature [34].

Potential drop  $\Delta E$  in Helmholtz layer equals  $(e\epsilon\epsilon_0 N_d)/(2C_H^2)$ . Since  $E_{fb} = E'_{fb} + \Delta E$ , we have first calculated  $C_H$  of the Helmholtz layer from dependence

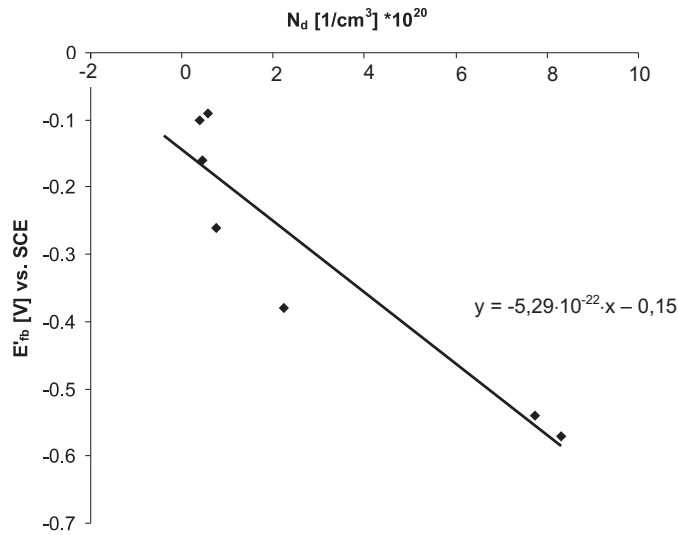


Fig. 7. Dependence  $E'_{fb} = f(N_d)$  for oxides formed in PBS solution

The slope of this dependence is equal  $(e\epsilon\epsilon_0)/(2C_H^2)$ . Next we used  $C_H$  to calculate a true value of flat band potential. The capacity of the Helmholtz layer was found to be equal to  $25.8 \mu\text{F}/\text{cm}^2$  for PBS solution and  $25.3 \mu\text{F}/\text{cm}^2$  for artificial saliva.

The donor densities, experimental values of flat band potential, corrected values of flat band potential are pre-

sented in tables 2a and 2b adequately for oxides formed in PBS and artificial saliva.

TABLE 2a

The donor densities, experimental values of flat band potential, corrected values of flat band potential for oxides formed in PBS solution

E[V] vs. SCE	$N_d [1/\text{cm}^3] \cdot 10^{20}$	$E'_{fb}$ [V] vs. SCE	$E_{fb}$ [V] vs. SCE
Stationary potential	7.72	-0.54	-0.131
0.2	8.32	-0.57	-0.129
1.5	2.22	-0.38	-0.255
3	0.75	-0.26	-0.218
5	0.46	-0.16	-0.136
7	0.39	-0.1	-0.079
9	0.58	-0.09	-0.059
average value of $E_{fb}$			<b>-0.144</b>

TABLE 2b

The donor densities, experimental values of flat band potential, corrected values of flat band potential for oxides formed in artificial saliva

E[V] vs. SCE	$N_d [1/\text{cm}^3] \cdot 10^{20}$	$E'_{fb}$ [V] vs. SCE	$E_{fb}$ [V] vs. SCE
Stationary potential	7.30	-0.66	-0.256
0.2	5.90	-0.62	-0.293
1.5	1.67	-0.5	-0.406
3	0.72	-0.35	-0.310
5	0.40	-0.28	-0.258
7	0.48	-0.26	-0.235
9	0.51	-0.265	-0.238
average value of $E_{fb}$			<b>-0.285</b>

From these tables we can see that donor density is decreasing when the potential of oxide forming is increasing. The flat band potential for oxide formed in PBS solution is equal  $-0.144$  V vs. SCE and for the layer formed in artificial saliva it is equal  $-0.285$  V vs. SCE.

## 5. Conclusions

The semiconductive properties of the titanium oxide films were investigated. It has been demonstrated that using EIS donor densities and flat band potentials can be determined. The donor densities and flat band potential values were calculated using Mott-Schottky equation. The values of donor densities presented in Tables 2a and 2b are characteristic of very thin oxide films, which are amorphous and with a lot of defects. Obtained donor densities for films grown in PBS solution and in artificial saliva are very similar, and in fact do not depend on pH of the solution. The values of donor

densities presented in this work are in good agreement with the data presented by other authors [16, 34, 35]. The donor density is a parameter which decides about the conductivity of a material. Thus, obtained results suggest that titanium oxide film is a n-type conductor. The Ti(III) and Ti(II) are believed to act as donors [36, 37] and this suggests that the mechanism of the growth of the thicker films is based on the migration of Ti ions towards the oxide/electrolyte interface [38].

The second parameter which was obtained from EIS measurements and Mott-Schottky plots is a flat band potential. This is one of the most important experimental parameters to measure on a semiconductor. The position of the band edges on the electrochemical scale, the direction of the band-bending and in favorable cases the magnitude of the band-bending can be determined if  $E_{fb}$  is known [16]. The values calculated from our measurements are comparable with the values of  $E_{fb}$  given in other studies [16, 34, 35]. The flat band potential depends on pH of the solution. Finklea presented in his work [16] the correlation with more than one hundred reported values of  $E_{fb}$  and plot all these data points vs variable pH. Our results correspond well to this correlation what is presented in Fig. 8.

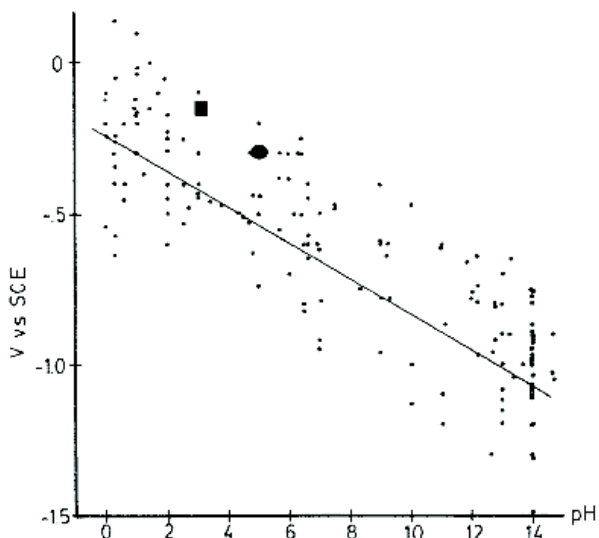


Fig. 8. Reported values of  $E_{fb}$  for  $\text{TiO}_2$  vs. pH compared with the values obtained in this work (■ – PBS pH = 2.9 and ● – artificial saliva pH = 5). The solid line is the standard potential for hydrogen evolution [16]

Electrical properties of titanium oxide film can find application in the fast growing field of nanotechnology. By adjusting electrochemical conditions of titanium anodization self-organized  $\text{TiO}_2$  films can be grown with the structure either amorphous or crystalline, and of different thickness and morphology [39]. Specific morphology of the oxide layer can be obtained in the

form of highly-ordered tubes, which may be used in the photovoltaic devices in solar cells. It was found that nanoporous photoelectrodes show significant improvement of solar-to-electrical conversion efficiency and consequently ordered  $\text{TiO}_2$  nanotube array can be used in hydrogen generation during water photoelectrolysis [40, 41]. Thus, it seems that gaining control over the anodization process, the old problem of the oxidation of metals may find unexpected application in the modern search of energy sources.

#### REFERENCES

- [1] T. Ohzuku, T. Hirai, *Electrochim. Acta* **27**, 1263 (1982).
- [2] P. Frach, D. Glob, K. Goedicke, M. Fahland, W.M. Gnehr, *Thin Solid Films* **445**, 251 (2003).
- [3] O. Treichel, V. Kirchhoff, *Surf. Coat. Technol.* **123**, 268 (2000).
- [4] T. Fuyuki, T. Kobayashi, H. Matsumami, *J. Electrochem. Soc.* **135**, 248 (1988).
- [5] L. Kavan, K. Kratochvilova, M. Grätzel, *J. Electroanal. Chem.* **394**, 93 (1995).
- [6] B. O'Regan, M. Grätzel, *Nature* **353**, 737 (1991).
- [7] Y. Li, J. Hagen, W. Schaffrath, P. Otschik, D. Haarer, *Solar Energy Mater. Solar Cells* **56**, 167 (1998).
- [8] B. Tryba, A.W. Morawski, M. Inagaki, *Appl. Catal.* **B 41**, 427 (2003).
- [9] J. Liu, D. Yang, F. Shi, Y. Cai, *Thin Solid Films* **429**, 225 (2003).
- [10] H. Oh, J. Lee, Y. Jeong, Y. Kim, Ch. Chi, *Surf. Coat. Technol.* **198**, 247 (2005).
- [11] A. Belaidi, S.M. Chaqour, O. Gorochoy, M. Neumann-Spallart, *Mater. Res. Bull.* **39**, 599 (2004).
- [12] G.K. Boschloo, A. Goosens, J. Schoonman, *J. Electrochem. Soc.* **144** (4), 1311 (1997).
- [13] S. Meyer, R. Gorges, G. Kreisel, *Thin Solid Films* **450**, 276 (2004).
- [14] Y. Lei, L.D. Zhang, J.C. Fan, *Chem. Phys. Lett.* **338**, 231 (2001).
- [15] G.K. Boschloo, D. Fitzmaurice, *J. Phys. Chem.* **B 103**, 7860 (1999).
- [16] H.O. Finklea, "Semiconductor electrodes", Elsevier, New York, (1988).
- [17] P. Silvester, "Electric Circuits", The Macmillan Press Ltd, Hong Kong, (1993).
- [18] K.S. Cole, R.H. Cole, *J. Chem. Phys.* **9**, 341 (1941).
- [19] J.E.B. Randles, *Discussions. Faraday Soc.* **1**, 11 (1947).
- [20] I. Epelboin, M. Keddam, H. Takenouti, *J. Appl. Electrochem.* **2**, 71 (1972).

- [21] I. Epelboin, M. Keddam, *J. Electrochem. Soc.* **117** (8), 1052 (1970).
- [22] R.D. Armstrong, M. Henderson, *J. Electroanal. Chem.* **39**, 81 (1972).
- [23] R.D. Armstrong, K. Edmondson, *Electrochim. Acta* **18**, 937 (1973).
- [24] M. Sluyters-Rehback, J.H. Sluyters, *Electroanal. Chem.* **4**, 1 (1969).
- [25] J.H. Sluyters, *Rec. Trav. Chim.* **79**, 1092 (1960).
- [26] K. Juttner, *Electrochim. Acta* **35** (10), 1501 (1990).
- [27] S.V. Gnedenkov, S.L. Sinebryukhov, V.I. Sergienko, *Russ. J. Electrochem.* **42** (3), 197 (2006).
- [28] B.A. Boukamp, *Solid State Ionics* **20**, 31 (1986).
- [29] <http://www.jrossmacdonald.com/levminfo.html>
- [30] <http://www.scribner.com/products/zplot/>
- [31] E. Barsoukov, J.R. Macdonald, "Impedance Spectroscopy – Theory, Experiment, and Applications", Wiley-Interscience, USA, (2005).
- [32] M. Pourbaix, "Atlas of Electrochemical Equilibria in Aqueous Solutions", NACE, (1974).
- [33] V. Macagno, J.W. Schultze, *J. Electroanal. Chem.* **180**, 157 (1984).
- [34] J. Pan, D. Thierry, C. Leygraf, *J. Biomed. Mat. Res.* **28**, 113 (1994).
- [35] A. Goossens, *Surf. Sci.* **365**, 662 (1996).
- [36] D.J. Blackwood, L.M. Peter, *Electrochim. Acta* **34**, 1051 (1989).
- [37] T. Ohtsuka, T. Otsuki, *Corr. Sci.* **40**, 951 (1998).
- [38] Y.Z. Huang, D.J. Blackwood, *Electrochim. Acta* **51**, 1099 (2005).
- [39] M. Macak, H. Tsuchiya, P. Schmuki, *Angew. Chem. Int. Ed.* **44**, 2100 (2005).
- [40] M. Paulose, K. Shankar, O.K. Varghese, G.K. Mar, B. Hardin, C.A. Grimes, *Nanotechnology* **17**, 1446 (2006).
- [41] Ch. Ruan, M. Paulose, O.K. Varghese, C.A. Grimes, *Solar Energy Mat. Solar Cells* **90**, 1283 (2006).